CHIN. PHYS. LETT. Vol. 29, No. 9 (2012) 090601

Magic Wavelengths for a Lattice Trapped Rubidium Four-Level Active Optical Clock *

ZANG Xiao-Run(臧孝润), ZHANG Tong-Gang(张同刚), CHEN Jing-Biao(陈景标)**

Institute of Quantum Electronics, and State Key Laboratory of Advanced Optical Communication System & Network, School of Electronics Engineering and Computer Science, Peking University, Beijing 100871

(Received 25 May 2012)

After being pumped from the $5s_{1/2}$ ground state to the $6p_{1/2}$ state, the population inversion between $6s_{1/2}$ and $5p_{1/2,3/2}$ can be established for a rubidium four-level active optical clock. We calculate the ac Stark shift due to lattice trapping laser which dominates the frequency shift of clock transition in a lattice trapped rubidium four-level active optical clock. Several magic wavelengths are found, which can form desired optical lattice trapping potential. By choosing a proper intensity and linewidth of the trapping laser, the fractional frequency uncertainty of clock transition due to the ac Stark shift of the trapping laser, is estimated to be below 10^{-18}.

PACS: 06.30.Ft, 32.10.Dk, 32.60.+i DOI: 10.1088/0256-307X/29/9/090601

Time or frequency precise measurement is extremely important for fundamental science and technology. An optical clock is, undoubtedly, the best time or frequency measurement instrument implemented to date.[1−3] The most accurate optical clock is an aluminium single-ion clock, which has achieved a fractional frequency uncertainty of 8.6×10^{-18}.[1] Although a single-ion optical clock possesses high accuracy, its stability is limited according to Allan variance, $\sigma_y(\tau) \propto 1/\sqrt{N}$.[4] Using neutral atoms trapped in an optical lattice is one way to break this limitation because it can greatly increase the total number of atoms.[5] Recently, a strontium optical lattice clock with 10^{-16} fractional uncertainty has been reported,[3,2] using the so-called magic wavelength trapping light to cancel the light shift of the two clock transition levels involved.[5] In such an optical lattice system, neutral atoms are trapped in the optical lattice and the trapped neutral atoms experience frequency shifts which arise from various mechanisms, i.e., trapping light shift, black-body shift, collision shift, first and second order Doppler shift, etc. In the Lamb-Dick regime,[6,7] collision shift and the first and second order Doppler shifts are greatly suppressed since their movements are confined. Therefore, most of the time, the first two terms will dominate the frequency shift.

However, both the single-ion trapped optical clock and the neutral-atom optical lattice clock mentioned above are working in passive modes, which are limited by the linewidth of the interrogating laser. On the other hand, an active optical clock[8−11] will output laser directly, whose frequency is determined by the optical clock transition. Therefore, it can provide two distinguishing qualities, i.e., a super-narrow quantum-limited linewidth and an extremely small cavity pulling shift.[9] Theoretically, a strontium clock using a thermal atomic beam implies a quantum-limited linewidth of 0.51 Hz and outshines state-of-the-art narrowest 6.7 Hz of the Hg single-ion clock and 1.5 Hz of the strontium optical lattice clock.[9] It promises to improve the stability of the best clocks by two orders of magnitude, and it can be extended to quenching laser and superradiant laser.[12−15]

The lattice trapped rubidium four-level active optical clock (Fig. 1) is a new experimental scheme to realize an active optical clock.

A population inversion exists between the clock transition $6s_{1/2}-5p_{1/2,3/2}$ with 8.4% in $6s_{1/2}$ and 3.3% in $5p_{3/2}$ when pumping from $5s$ to $6p_{1/2}$ with a laser of 421.7 nm wavelength and 318 mW/cm^2 intensity.[16] The population inversion is formed after 10^{-6} s, thus a steady photon number will be sustained with a bad cavity to form an active optical clock. Even considering the Rayleigh scattering and Raman scattering in the optical lattice, a trap lifetime larger than 100 s is still achievable,[17−19] and such a long period is sufficient for a lattice trapped rubidium four-level active optical clock. In this study, we derive several magic wavelengths for such a system.

Neutral rubidium can be cooled and trapped in an optical lattice due to dipole gradient force.[20−22] The trapping light, meanwhile, causes a light shift of energy levels, which is affected by both the wavelengths and the intensities of the trapping light.

According to quantum perturbation theory, the energy shift of the arbitrary state can be expressed as

$$\Delta E = -\frac{1}{2}(E)^2 \alpha_J^{(2)}, \tag{1}$$

where E is the electric field strength, $\alpha_J^{(2)}$ is the polarizability of related states. We concentrate on the

*Supported by the National Natural Science Foundation of China under Grant Nos 10874009 and 11074011.

**Corresponding author. Email: jbchen@pku.edu.cn

© 2012 Chinese Physical Society and IOP Publishing Ltd

electric dipole interaction and neglect all higher-order perturbations.

Table 1. Neutral rubidium energy levels in wavelength (nm) and electric-dipole matrix elements in (a.u.). For the $5p_{1/2}$ and $5p_{3/2}$ states, transitions to $5s$, $6s$, $7s$, $8s$ and to $4d$, $5d$, $6d$ are included, and for the $6s_{1/2}$ state, transitions to $5p$, $6p$, $7p$, $8p$ are included.

Transition	wavelength (nm)	RMEs (a.u.)
$5p_{1/2}$–$5s_{1/2}$	794.98[a]	4.231[a]
	794.979[b]	4.221[c]
$5p_{1/2}$–$6s_{1/2}$	1323.88[a]	4.146[a]
$5p_{1/2}$–$7s_{1/2}$	728.20[a]	0.953[a]
$5p_{1/2}$–$8s_{1/2}$	607.24[a]	0.502[a]
$5p_{1/2}$–$4d_{3/2}$	1475.65[a]	8.051[a]
$5p_{1/2}$–$5d_{3/2}$	762.10[a]	1.35[a]
$5p_{1/2}$–$6d_{3/2}$	620.80[a]	1.07[a]
$5p_{3/2}$–$5s_{1/2}$	780.24[a]	5.977[a]
	780.241[b]	5.956[c]
$5p_{3/2}$–$6s_{1/2}$	1366.87[a]	6.05[a]
$5p_{3/2}$–$7s_{1/2}$	741[a]	1.35[a]
$5p_{3/2}$–$8s_{1/2}$	616.13[a]	0.708[a]
$5p_{3/2}$–$4d_{3/2}$	1529.26[a]	3.63[a]
$5p_{3/2}$–$4d_{5/2}$	1529.37[a]	10.9[a]
$5p_{3/2}$–$5d_{3/2}$	776.16[a]	0.67[a]
$5p_{3/2}$–$5d_{5/2}$	775.98[a]	1.98[a]
$5p_{3/2}$–$6d_{3/2}$	630.1[a]	0.51[a]
$5p_{3/2}$–$6d_{5/2}$	630.01[a]	1.51[a]
$6s_{1/2}$–$5p_{1/2}$	1323.88[b]	4.119[c]
$6s_{1/2}$–$6p_{1/2}$	2791.29[b]	9.684[c]
$6s_{1/2}$–$7p_{1/2}$	1298.28[b]	0.999[c]
$6s_{1/2}$–$8p_{1/2}$	1030.67[b]	0.393[c]
$6s_{1/2}$–$5p_{3/2}$	1366.87[b]	6.013[c]
$6s_{1/2}$–$6p_{3/2}$	2732.18[b]	13.592[c]
$6s_{1/2}$–$7p_{3/2}$	1292.39[b]	1.54[c]
$6s_{1/2}$–$8p_{3/2}$	1028.67[b]	0.628[c]

[a]Ref. [23]. [b]Refs. [24,25]. [c]Ref. [26].

We consider the linearly polarized light to exclude the axial polarizability associated with light polarization and choose the orientation of the trapping light polarization along the magnetic z-axis, and finally the polarizability expression is written as[23]

$$\alpha_J^{(2)} = \alpha_J^{S,(2)} + \frac{3m_j^2 - J(J+1)}{J(2J-1)}\alpha_J^{T,(2)}, \qquad (2)$$

where $\alpha_J^{S,(2)}$ and $\alpha_J^{T,(2)}$ represent the scalar and tensor polarizabilities, and all the variables and signs follow Ref. [23].

All reduced matrix elements (RMEs) and energy levels needed in our calculation are listed in Table 1.

Part of the RMEs are derived from the equation $d^2 = 3c^3W(1+2J)/(4\omega^3)$, where d is the reduced matrix element, W is the transition probability, J is the total angular momentum quantum number. The above equation has used atomic units, where $m_e = \hbar = e = \frac{1}{4\pi\epsilon_0} = 1$.

To verify the validity of our calculation for the rubidium atom we reproduce some calculations from Ref. [23], then we calculate the ac polarizabilities of $5p_{1/2}$, $5p_{3/2}$ and $6s_{1/2}$ using Eq. (2).

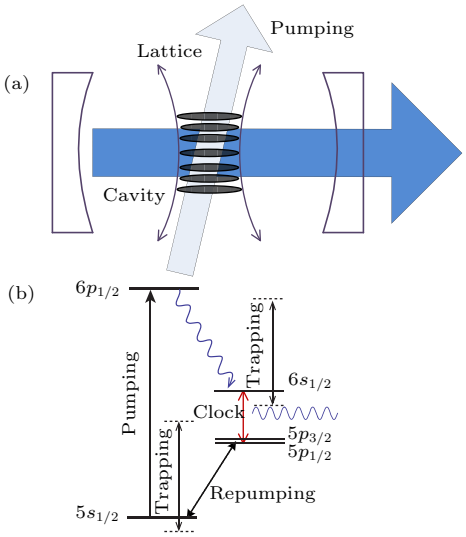

Fig. 1. Scheme of the lattice trapped rubidium four-level active optical clock, with 421.7 nm pumping light to pump neutral rubidium from ground state $5s_{1/2}$ to the excited state $6p_{1/2}$ and 780 nm, 795 nm repumping light to repump atoms back to the optical loop. A population inversion between $6s$ and $5p$ states is formed with time evolution, and atoms are trapped in the optical lattice clock at a magic wavelength where the light frequency shift of the clock transition arising from the trapping light is cancelled.

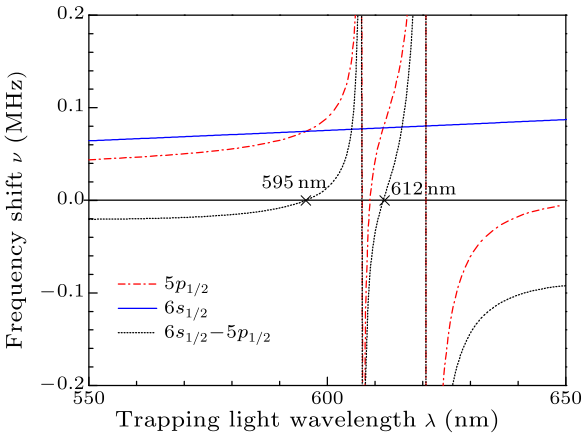

Fig. 2. The frequency shift of the states $5p_{1/2}$ (red dot-dashed line) (red) and $6s_{1/2}$ (blue solid line) with the assumption that the intensity of trapping laser is 10 kW/cm^2. The different frequency shifts go to zero at a magic wavelength, which is marked as cross symbol.

The polarizability of $6s_{1/2}$ results from the summation of all the levels that have electric-dipole interactions with $6s_{1/2}$. The transition frequencies np–$6s$ can be readily obtained from the NIST website[25] and other related papers,[24] the reduced electric-dipole moment values are from Safronova *et al.*[26] who calculated the reduced electric-dipole moments up to $8p$–$6s$

using a relativistic all-order method. Using these values to calculate the polarizability of the $6s$ state is enough for a rough evaluation, and we will discuss the accuracy at the end.

Figures 2 and 3 show the different frequency shifts between $6s_{1/2}$ and $5p_{1/2}$ levels while the trapping light frequency varies from 550 nm to 650 nm, 1200 nm to 1600 nm. The light shift of $5p_{1/2}$ is dominated by the electric dipole interaction $5p_{1/2}$–$8s_{1/2}$ at wavelength 595 nm, which is lower than the resonance wavelength. At wavelength 612 nm, $5p_{1/2}$ is greatly shifted by two electric dipole interactions $5p_{1/2}$–$8s_{1/2}$ and $5p_{1/2}$–$6d_{3/2}$. Two magic wavelengths 1342 nm and 1421 nm are found between 1200 nm and 1600 nm.

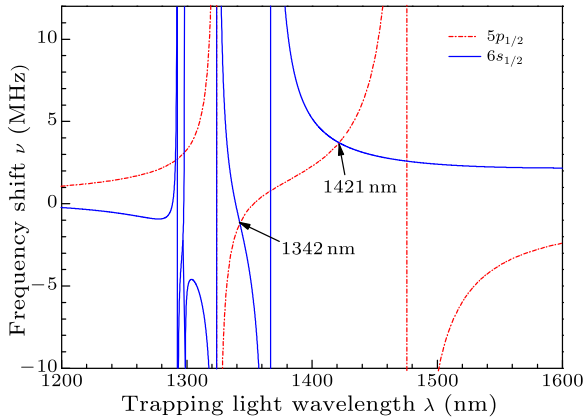

Fig. 3. The frequency shift of the states $5p_{1/2}$ (red dot-dashed line) (red) and $6s_{1/2}$ (blue solid line) with the assumption that the intensity of trapping laser is 10 kW/cm^2.

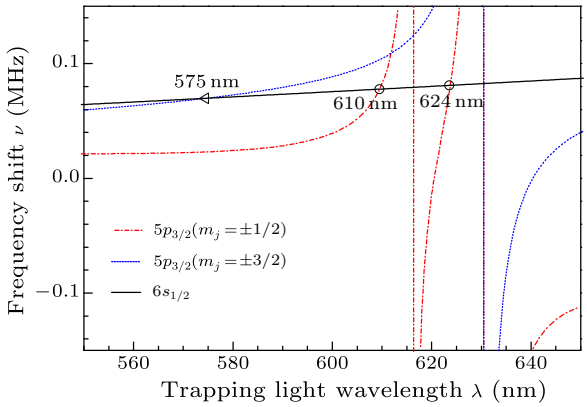

Fig. 4. The frequency shift of the states $5p_{3/2}(m_j = \pm\frac{1}{2})$ (red dot-dashed line), $5p_{3/2}(m_j = \pm\frac{3}{2})$ (blue dotted line) and $6s_{1/2}$ (black solid line) with the assumption that the intensity of trapping laser is 10 kW/cm^2. Light shifts of the states $5p_{3/2}(m_j = \pm\frac{1}{2})$ and $6s_{1/2}$ intersect at the magic wavelength, which is marked by a circle symbol. The triangle symbol marks the cross point of light frequency shift of states $5p_{3/2}(m_j = \pm\frac{3}{2})$ and $6s_{1/2}$.

Figures 4 and 5 show the different frequency shifts between the $6s_{1/2}$ and $5p_{3/2}$ levels while the trapping light frequency varies from 550 nm to 650 nm, 1200 nm to 1600 nm. With respect to the state $5p_{3/2}(|m_j| = \frac{1}{2})$, the wavelength 610 nm is lower than the resonance $5p_{3/2}$–$8s_{1/2}$ wavelength, while wavelength 624 nm is between the resonance $5p_{3/2}$–$8s_{1/2}$ and resonance $5p_{3/2}$–$6d_{3/2}$. For the state $5p_{3/2}(|m_j| = \frac{3}{2})$, the wavelength 575 nm lies on the blue side of the resonance $5p_{3/2}$–$6d_{3/2,5/2}$. For optical clock transition $6s_{1/2}$–$5p_{3/2}(|m_j| = \frac{1}{2})$, 1331 nm and 1461 nm are magic wavelengths; for $6s_{1/2}$–$5p_{3/2}(|m_j| = \frac{1}{2})$, two magic wavelengths 1336 nm and 1453 nm are found.

Magic wavelengths in the ranges of 550–650 nm and 1200–1600 nm are listed in Table 2. The frequency uncertainties at each magic wavelength are listed in Table 3 by properly adjusting trapping laser intensities, i.e., trapping depths.

Table 2. The magic wavelengths for optical clock transitions $6s_{1/2}$–$5p_{1/2}$ and $6s_{1/2}$–$5p_{3/2}$ and lattice trapping depths to the intensity of lattice laser $\Delta\nu/I$ (kHz·kW^{-1}cm^{-2}) referring to those magic wavelengths listed.

$6s_{1/2}$–$5p_{1/2}$		$6s_{1/2}$–$5p_{3/2}$	
λ (nm)	$\Delta\nu/I$ (kHz·kW^{-1}cm^{-2})	λ (nm)	$\Delta\nu/I$ (kHz·kW^{-1}cm^{-2})
595	−74.5	575	−69.7
612	−78.2	610	−77.7
1342	1196.7	624	−81.0
1421	−3707.2	1331	−4453.4
		1336	−995.2
		1453	−2878.1
		1461	−2753.4

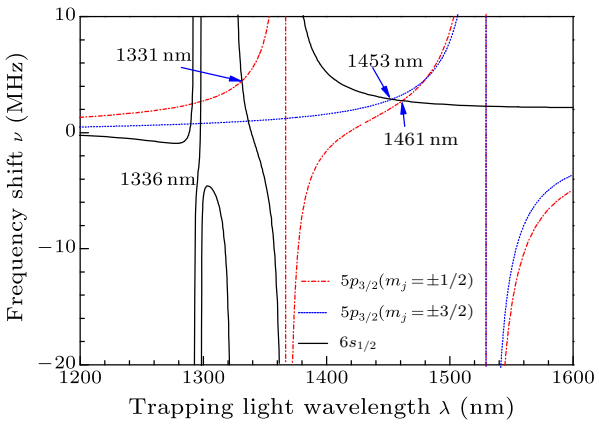

Fig. 5. The frequency shift of the states $5p_{3/2}(m_j = \pm\frac{1}{2})$ (red dot-dashed line), $5p_{3/2}(m_j = \pm\frac{3}{2})$ (blue dotted line) and $6s_{1/2}$ (black solid line) with the assumption that the intensity of trapping laser is 10 kW/cm^2. Light shifts of the states $5p_{3/2}(m_j = \pm\frac{1}{2})$ and $6s_{1/2}$ intersect at the magic wavelength marked by a circle symbol. The triangle symbol marks the cross point of light frequency shift of states $5p_{3/2}(m_j = \pm\frac{3}{2})$ and $6s_{1/2}$.

The reasons for choosing the four-level quantum system rather than three-level, and an optical lattice clock rather than a thermal atomic beam are as follows. For a thermal atomic beam clock, the residual Doppler shift will be extremely large, however an optical lattice clock removes the effect since atoms are laser cooled and trapped in the Lamb–Dick regime. On the other hand, a three-level system is affected by the light shift of the pumping laser. The four-level

quantum system, however, can avoid such disadvantage by choosing clock transition without involving the ground state, which is connected to the pumping laser directly.

In our calculation, we use the reduced matrix element data up to $8p$–$6s$ transition. Since the frequency shifts of $6s$ due to $8p_{1/2}$ and $8p_{3/2}$ states contribute less than 0.081%, at all magic wavelengths, to the total polarizability of $6s$, we therefore believe that states above $8p$ will contribute less. For the polarizability of $5p_{1/2}$, states $5s_{1/2}$, $6s_{1/2}$ and $4d_{3/2}$ will dominate, states $8s_{1/2}$ and $6d_{3/2}$ in total have less than 0.639% effect.

In conclusion, four magic wavelengths 595 nm, 612 nm, 1342 nm and 1421 nm are available for transition $6s_{1/2}$–$5p_{1/2}$, seven magic wavelengths 575 nm, 610 nm, 624 nm, 1331 nm, 1336 nm, 1453 nm and 1461 nm are candidates for transition $6s_{1/2}$–$5p_{3/2}$ (listed in Table 2). To obtain a 10^{-18} fractional uncertainty or even less, one must well control the linewidth of the lattice laser, i.e., below 10 kHz as listed in Table 3. With respect to magic wavelengths between 550 nm and 650 nm, a further discussion is needed since those wavelengths are going above the ionization limit of $6s_{1/2}$ (741 nm). In addition, dynamic stark shift induced by black-body radiation will be discussed elsewhere.

Table 3. Adjusting the intensities I (W/cm^2) of the trapping laser to provide sufficient trapping depths $\Delta\nu$ (kHz). For each magic wavelength λ (nm) the frequency uncertainties (mHz) due to lattice laser frequency fluctuation (assumed to be 10 kHz) are listed.

λ (nm)	I (W/cm^2)	$\Delta\nu$ (kHz)	Uncertainty (mHz)
595	1×10^4	−745	4.3×10^{-4}
612	1×10^4	−782	4.6×10^{-4}
1342	1×10^3	1196.7	3.2×10^{-1}
1421	200	−741.4	9.0×10^{-3}
575	1×10^4	−697	3.9×10^{-4}
610	1×10^4	−777	4.6×10^{-4}
624	1×10^4	−810	4.8×10^{-4}
1331	200	−890.7	2.0×10^{-1}
1336	1×10^3	−995.2	4.2×10^{-1}
1453	250	−863.4	4.6×10^{-3}
1461	250	−688.4	3.8×10^{-3}

Moreover, the pumping light of wavelength 421.7 nm and intensity 318 mW/cm^2 contributing frequency corrections to optical clock transitions of $6s_{1/2}$–$5p_{1/2}$, $6s_{1/2}$–$5p_{3/2}(m_j = \pm\frac{1}{2})$, $6s_{1/2}$–$5p_{3/2}$ $(m_j = \pm\frac{3}{2})$ are 0.45 Hz, 0.65 Hz and 0.28 Hz, respectively and related uncertainties will be no more than 1 mHz when an order of 10^{-3} intensity fluctuation of pumping laser is considered. Although our results are specified for the rubidium atom, they are ready to be generalized to other alkaline atoms.

The authors thank Xiaoji Zhou, Xia Xu and Anpei Ye for discussions.

References

[1] Chou C W, Hume D B, Koelemeij J C J, Wineland D J andRosenband T 2010 *Phys. Rev. Lett.* **104** 070802
[2] Katori H 2011 *Nat. Photon.* **5** 203
[3] Ludlow A D et al 2008 *Science* **319** 1805
[4] Allan D W 1966 *Proc. IEEE* **54** 221
[5] Katori H, Takamoto M, Pal'chikov V G and Ovsiannikov V D 2003 *Phys. Rev. Lett.* **91** 173005
[6] Dicke R H 1953 *Phys. Rev.* **89** 472
[7] Ido T and Katori H 2003 *Phys. Rev. Lett.* **91** 053001
[8] Chen J and Chen X 2005 *Proceedings of International Frequency Control Symposium* (IEEE, Vancouver, BC 2005) p 608
[9] Chen J 2009 *Chin. Sci. Bull.* **54** 348
[10] Wang Y 2009 *Chin. Sci. Bull.* **54** 347
[11] Yu D and Chen J 2008 *Phys. Rev.* A **78** 013846
[12] Meiser D, Ye J, CarlsonD R and Holland M J 2009 *PhysRev. Lett.* **102** 163601
[13] Yu D and Chen J 2010 *Phys. Rev.* A **81** 023818
[14] Yu D and Chen J 2010 *Phys. Rev.* A **81** 053809
[15] Bohnet J G and et al 2012 *Nature* **484** 78
[16] Zhang T, Wang Y, Zang X, Zhuang W and Chen J 2012 arXiv:1204.4385v1 [physics.atom-ph]
[17] O'Hara K M, Granade S R, Gehm M E, Savard T A Bali S, Freed C and Thomas J E 1999 *Phys. Rev. Lett.* **82** 4204
[18] O'Hara K M, Granade S R, Gehm M E and Thomas J E 2001 *Phys. Rev.* A **63** 043403
[19] Zhou X, Chen X, Chen J, Wang Y and Li J 2009 *Chin. Phys. Lett.* **26** 090601
[20] Letokhov V S 2007 *Laser Control of Atoms and Molecules* (Oxford: Oxford University Press)
[21] Westbrook C I, Watts R N, Tanner C E, Rolston S L, Phillips W D, Lett P D and Gould P L 1990 *Phys. Rev. Lett.* **65** 33
[22] Metcalf H J and van der Straten P 1999 *Laser Cooling and Trapping* (Berlin: Springer-Verlag)
[23] Arora B, Safronova M S and Clark C W 2007 *Phys. Rev.* A **76** 052509
[24] Sansonetti J E 2006 *J. Phys. Chem. Ref. Data* **35** 301
[25] Ralchenko Y, Kramida A, Reader J and NIST ASD Team 2011 *NIST Atomic Spectra Database* (version 4.1) http://physics.nist.gov/asd
[26] Safronova M S, Williams C J and Clark C W 2004 *Phys. Rev.* A **69** 022509